The mechanism of methanol loss from the $(M - H)^-$ ions of *cis*- and *trans*-4-methoxycyclohexanol. The application of experiment and theory in concert

Suresh Dua, Mark A. Buntine, Mark J. Raftery, Peter C. H. Eichinger and John H. Bowie

Department of Chemistry, The University of Adelaide, South Australia, 5005

Deprotonation of *cis*- and *trans*-4-methoxycyclohexanol by HO^- in the ion source of a mass spectrometer yields the $(M - H)^-$ alkoxide ions exclusively. Both of these ions, on collisional activation, form MeO^-, $MeO^-(H_2O)$ and eliminate MeOH. The loss of methanol forms the base peak of the spectrum, and the structure of this daughter anion is shown to be the alkoxide ion from cyclohex-3-enol for both isomers. Evidence (based on product ion, deuterium labelling and AM1 semiempirical computational studies) indicates that the loss of methanol from the *trans* isomer proceeds by an internal S_N2 cyclisation of O^- at the four position (through a 1,4-epoxycyclohexane species) followed by 3,4 elimination. A similar sequence may occur for the *cis*-isomer, but in this case the process is not as energetically favourable as that for the *trans* isomer.

Introduction

Charge-remote mass spectrometric fragmentations are those which take place remote from and uninfluenced by the charged centre. Such processes are well known for positive ions, but less so for negative ions.[1,2] The classical proposal for negative ions is shown in eqn. (1):[1,2] this is a high-energy process,[2] and a recent elegant study[3] has substantiated the formation of a neutral olefin by this process. Even-electron organic anions fragment preferentially by loss of a neutral molecule, but simple cleavage resulting in the loss of a radical may also occur.[4] Simple cleavages involving loss of a radical are often 'remote': generally such reactions produce particularly stable radical anions. Examples of such processes are shown in eqns. (2) and (3).[5]

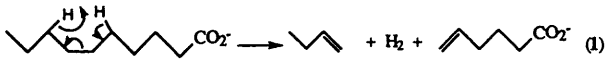

(1)

$$RC(O)^-CHOMe \longrightarrow (RCOCHO)^{-\bullet} + MeO\bullet \quad (2)$$

$$CH_3COCH_2^- \longrightarrow (CH_2COCH_2)^{-\bullet} + H\bullet \quad (3)$$

$$^-C{\equiv}C\text{-}CH_2\text{-}OMe \longrightarrow [(:C{=}C{=}CH_2)^-OMe] \longrightarrow C_3H^- + MeOH \quad (4)$$

In contrast, we have not been able to substantiate the operation of 'remote' processes involving the loss of neutral molecules (non-radicals) from simple organic anions. In all cases that we have studied to date, there has been a lower energy pathway more favourable than the anticipated 'remote' process. A particular example concerns the loss of methanol from $^-C{\equiv}CCH_2OMe$ which we predicted would involve a synchronous four-centre elimination with no participation from the anion centre: the loss of methanol is indeed the major process, but it occurs as shown in eqn. (4).[6,cf.7]

There are some situations where it is not possible to distinguish experimentally between a 'remote' process and one which involves proton transfer to the initial anion site to form a new anion which then directs the fragmentation. There are a number of cases of this scenario for the characteristic decompositions of deprotonated peptides: the loss of cinnamic acid from peptides containing *C*-terminal Phe illustrates the problem [see eqn. (5) for the 'remote' process, and eqn. (6) for the 'anionic' mechanism].[8]

The loss of methanol from deprotonated *trans*-2-methoxycyclohexanol occurs exclusively following epoxide

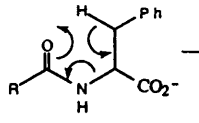

$$\longrightarrow PhCH{=}CHCO_2^- + RC(OH){=}NH \quad (5)$$

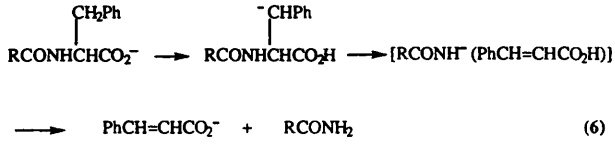

$$\longrightarrow PhCH{=}CHCO_2^- + RCONH_2 \quad (6)$$

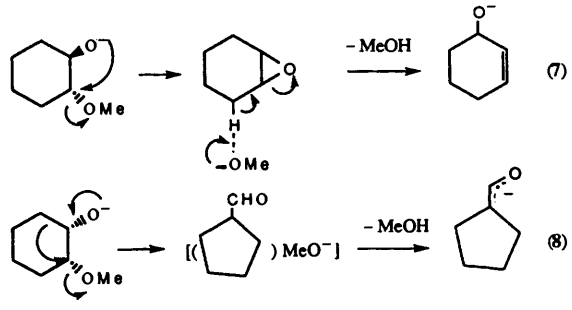

(7)

(8)

formation [eqn. (7)], while the *cis* isomer loses methanol by a negative ion pinacol rearrangement [eqn. (8)].[9] The fact that these two stereoisomers fragment quite differently led us to enquire as to the fragmentation behaviour of the $(M - H)^-$ ions of the related *cis*- and *trans* 4-methoxycyclohexanol. In these cases, the charged centre (O^-) and the methoxy substituent are no longer adjacent. This paper addresses the following questions: *viz.* (*i*) do the $(M - H)^-$ ions of these two isomers fragment by loss of methanol, and (*ii*) if they do, could this loss of methanol be a 'remote' process?

Results and discussion

The loss of methanol from deprotonated *cis*- and *trans*-4-methoxycyclohexanol—mechanistic possibilities

First, it is necessary to determine the deprotonation centre(s) of the 4-methoxycyclohexanols. Thus we prepared *cis*- and *trans*-

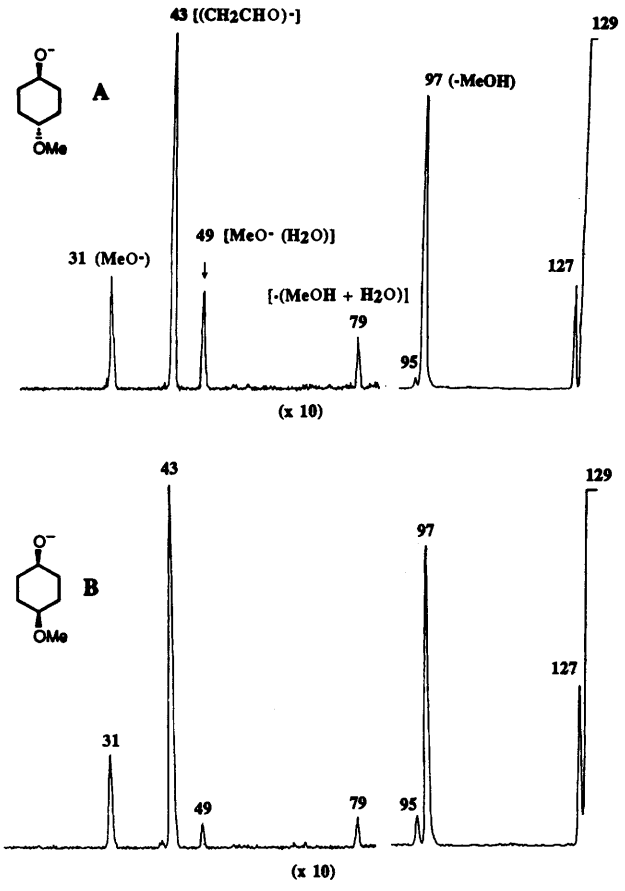

Fig. 1 Collision-induced negative ion chemical ionisation mass spectra (MS/MS) of the $(M - D)^-$ parent ions of (**A**) *trans*-4-methoxycyclohexanol (OD) and (**B**) *cis*-4-methoxycyclohexanol (OD). ZAB 2HF mass spectrometer. For experimental details see the Experimental section.

4-methoxycyclohex-3-enol (OD) and allowed each to react with DO^- in the ion source of the VG ZAB 2HF instrument. $(M - D)^-$ ions were formed exclusively.

The collision-induced tandem mass spectra (MS/MS) of the two $(M - D)^-$ parent ions are shown in Fig 1. The spectra show pronounced peaks corresponding to loss of methanol. Both spectra are visually similar apart from differences in the relative abundances of certain peaks. However there is a further, and very important difference between the two spectra. The widths at half height of the peaks produced by loss of methanol are significantly and reproducibly different (23.1 ± 0.2 V for the *trans* isomer; 29.6 ± 0.2 V for the *cis* isomer). Relative peak widths provide information concerning the energetics of processes (particularly the reverse activation energies) and/or the structures of the product ions.[10] In this particular case the experimental observation suggests either that (*i*) the structures of the two product ions are different, or (*ii*) the structures are the same but the mechanisms (or energies) of formation of the ions are different.

Without considering any further data, we suggest four possible processes which might account for the losses of methanol from the two isomeric parent anions. These are detailed below, and summarized in Scheme 1.

(*A*) A fundamental fragmentation of any alkoxide ion (containing at least one hydrogen attached to the α-carbon) proceeds *via* a hydride ion complex.[11] The ion complex may undergo a variety of processes, the most common of which is deprotonation to liberate H_2. In the present case, the incipient hydride ion does induce loss of H_2, but we suggest that it also may displace MeO^- by an internal S_N2 process [*anti* attack of H^- (for the *cis* isomer) should be kinetically favoured] as

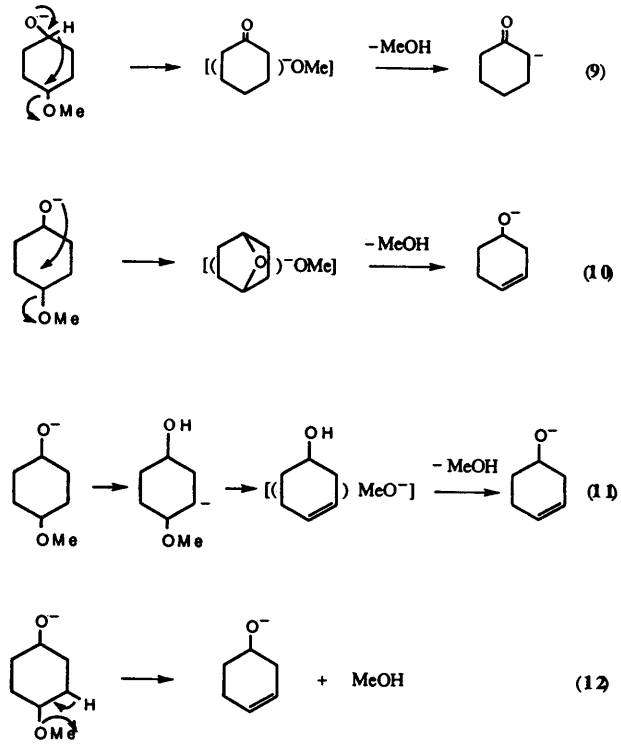

Scheme 1

summarized in sequence (9), with subsequent deprotonation yielding deprotonated cyclohexanone.

(*B*) The second possibility involves an initial cross ring S_N2 cyclisation [sequence (10)]: the *anti* reaction (for the *trans* isomer) should be favoured kinetically. There is a condensed phase analogy for this proposal: *viz.* (*i*) alkaline hydrolysis of *trans*-4-chlorocyclohexanol proceeds through 1,4-epoxycyclohexane to yield cyclohex-3-enol.[12]

(*C*) The third possibility [sequence (11)] involves a proton transfer to form a transient E1cb species which undergoes elimination followed by deprotonation [*anti* elimination (from the *trans* isomer) should be favoured kinetically].

(*D*) The remote mechanism shown in sequence (12) is the final possibility. The process should not be influenced by the charged site. The activation energy for the *syn* elimination of methanol through a four-centre transition state should be similar for both *cis* and *trans* isomers. As far as we are aware, there is no direct analogy for this process in the condensed phase. The closest analogy involves the heating of cyclohexyl acetate which results in *syn* elimination of acetic acid (but through a six-membered transition state), yielding cyclohexene in high yield.[13]

The structures of the product ions

The next phase of this investigation required the determination of the structures of the ions formed by the losses of methanol from the stereoisomeric $(M - H)^-$ ions. The two possibilities shown in Scheme 1 are the $(M - H)^-$ ions derived from cyclohexanone and cyclohex-3-enol. These two ions were synthesised by deprotonation of the appropriate neutrals in the ion source using HO^-, and their mass spectra are recorded in Fig. 2. Both spectra show characteristic fragmentations: deprotonated cyclohexanone fragments competitively by loss of H_2 and the elimination of ethene,[14] while deprotonated cyclohex-3-enol loses H_2O and H_2 and forms the acetaldehyde enolate ion [eqns. (13)–(15) (Scheme 2)]. We have obtained (*i*) tandem MS/MS/MS data for the two *m/z* 97 ions formed from the $(M - H)^-$ ions of *cis*- and *trans*-4-methoxycyclohexanol (using a tandem MS 50 TA instrument), and (*ii*) the MS/MS data (using the VG ZAB 2HF instrument) for source-formed *m/z* 97 ions. All four spectra (listed in Table 1) are very similar, and correspond to the

Table 1 CID MS/MS data for [(M − H)$^-$ − MeOH] ions from *cis*- and *trans*-4-methoxycyclohexanol [*m/z* (loss or formation) relative abundance]

cis Isomer	MS/MS[a]	95 (H_2) 28, 79 (H_2O) 12, 43 ($^-CH_2CHO$) 100, 41 (HC_2O^-) 1
	MS/MS/MS[b]	95 (H_2) 22, 79 (H_2)O 10, 43 ($^-CH_2CHO$) 100
trans Isomer	MS/MS[a]	95 (H_2) 26, 79 (H_2O) 11, 43 ($^-CH_2CHO$) 100, 41 (HC_2O^-) 1
	MS/MS/MS[b]	95 (H_2) 20, 79 (H_2O) 10, 43 ($^-CH_2CHO$) 100

[a] Source-formed ion, VG ZAB 2HF instrument. [b] MS 50 TA instrument.

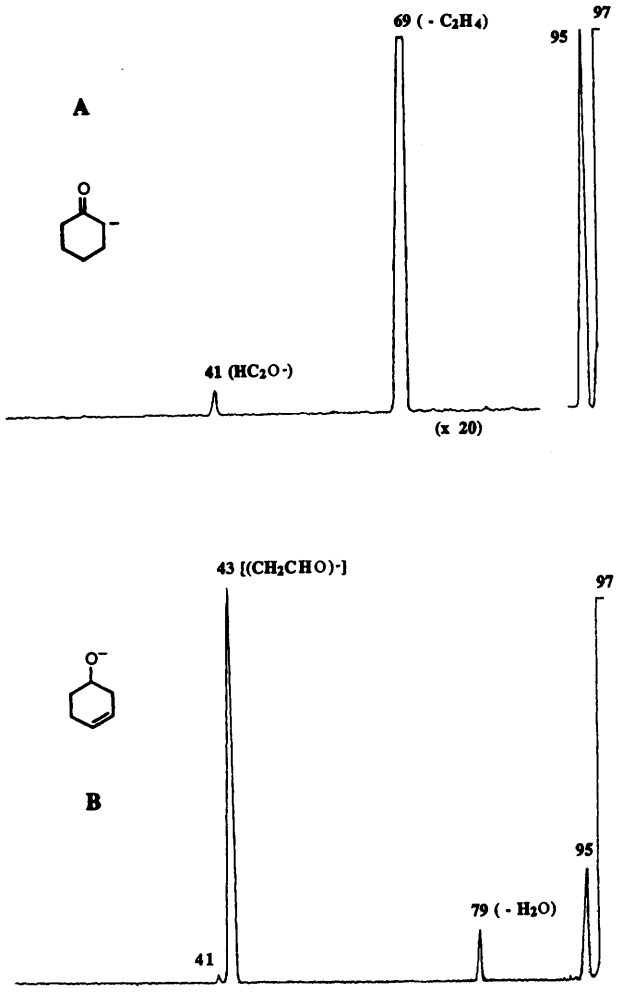

Fig. 2 Collision-induced negative ion chemical ionisation mass spectra (MS/MS) of deprotonated (**A**) cyclohexanone, and (**B**) cyclohex-3-enol. ZAB 2HF mass spectrometer.

spectrum of the (M − H)$^-$ ion from cyclohex-3-enol.† Thus the product ions resulting from loss of methanol are identical for both isomers, and process (9) (Scheme 1) cannot be operative.

Identification of the deprotonation centre for methanol loss

Having determined the structures of the product ions resulting from loss of methanol, it is now necessary to determine which hydrogen is lost in the deprotonation process. In order to do this, we have synthesised the neutrals **16–19** by the routes outlined in the Experimental section. The spectra of the (M − H)$^-$ ions of **16–19** are recorded in Table 2, as are the spectra of the source-formed [(M − H)$^-$ − MeOH] ions from **16** and **17**, and the [(M − H)$^-$ − MeOD] ions from **18** and **19**.

The following observations follow from the spectra (Table 2) of the (M − H)$^-$ ions of **16–19**. (*i*) The (M − H)$^-$ ions from **16** and **17** lose only MeOH. The spectrum of the [(M − H)$^-$ − MeOH] ions from **16** and **17** are those of deprotonated [1-^{2}H]cyclohex-3-enol and [2,2,6,6-$^2H_4$]cyclohex-3-enol, respectively. (*ii*) The (M − H)$^-$ ions from **18** and **19** lose MeOD exclusively, the widths of the [(M − H)$^-$ − MeOD] peaks at half height are 23.0 ± 0.2 V (*trans* isomer, **19**) and 29.1 ± 0.2 V (*cis* isomer, **18**), and the spectra of both [(M − H)$^-$ − MeOD] ions are those of deprotonated [3,5,5-$^2H_3$]cyclohex-3-enol. Thus the loss of MeOH from both of the unlabelled *cis* and *trans* parent ions involves a 3 (5) H, and the product ion (in each case) is deprotonated cyclohex-3-enol.

† The basic fragmentations of deprotonated cyclohex-3-enol can also be seen in the spectra illustrated in Fig. 1 (*viz.*, *m/z* 95, 79 and 43; *cf.*, Fig. 2).

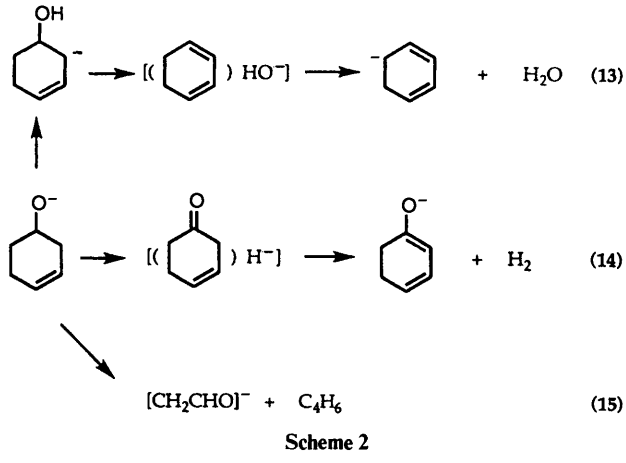

Scheme 2

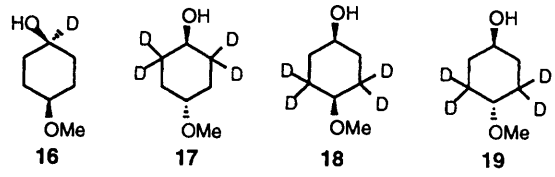

The formation of [MeO$^-$(H$_2$O)]

The experimental evidence for the loss of MeOH, to date, can be accommodated by any of the mechanisms (10), (11) or (12) (Scheme 1). However, there is a further piece of evidence which needs to be taken into account when considering the mechanism of methanol loss. Both of the spectra in Fig. 1 show peaks at *m/z* 49, which correspond to the hydrated methoxide anion [MeO$^-$(H$_2$O)]. This is confirmed by the mass spectrum of source-formed *m/z* 49 which shows loss of water to form MeO$^-$. The ion [MeO$^-$(H$_2$O)] is also formed from the $^2H_1$ derivative **16**, whereas the (M − H)$^-$ parent ions of the $^2H_4$ derivatives **17–19** fragment to give *m/z* 50 [MeO$^-$(HOD)]. We have not observed such a cluster ion in studies of cognate systems, even when hydroxy and methoxy substituents are on adjacent carbon atoms.[9,15] The solvated ions must be formed *via* an intermediate in which the two oxygen atoms are in close proximity.

The probability is that there is only one reactive intermediate which is involved in the loss of methanol, and the formation of both the methoxide and the hydrated methoxide anions from each isomer. Such an intermediate cannot be formed during either the remote process (12) or the proton transfer process (11), because in these cases, the two oxygen-containing substituents do not approach each other. However, close approach of these interacting substituents can, in principle, occur during cyclisation process (10).

Table 2 CID MS/MS data for $(M - H)^-$ ions from deuteriated compounds **16–19**, and for $[(M - H)^- - MeOH]$ from (**16**, **17**) and $[(M - H)^- - MeOD]$ ions from **18**, and **19** [*m/z* (loss or formation) relative abundance]

16 $(M - H)^-$	127 (HD) 30, 98 (MeOH) 100, 95 (HD + MeOH) 8, 80 (MeOH + H_2O) 1, 49 [$MeO^-(H_2O)$] 1, 44 (^-CHDCHO) 12, 31 (MeO^-) 2
17 $(M - H)^-$	130 (HD) 18, 101 (MeOH) 100, 97 (HD + MeOD) 3, 82 (MeOH + HOD) 2, 81 (MeOH + D_2O) 1, 50 [MeO^-(HOD)] 2, 45 ($^-CD_2CHO$) 5, 31 (MeO^-) 2
18 $(M - H)^-$	131 (H_2) 42, 100 (MeOD) 100, 99 (H_2 + MeOH) < 10,[a] 82 (MeOH + HOD) 2, 81 (MeOH + D_2O) 1, 50 [MeO^-(HOD)] 1, 43 ($^-CH_2CHO$) 10, 31 (MeO^-) 2
19 $(M - H)^-$	131 (H_2) 30, 100 (MeOD) 100, 99 (H_2 + MeOH) < 10,[a] 82 (MeOH + HOD) 1, 81 (MeOH + D_2O) 0.5, 50 [MeO^-(HOD)] 2.5, 43 ($^-CH_2CHO$) 12, 31 (MeO^-) 3
16 $[(M - H)^- - MeOH]$	95 (HD) 8, 80 (H_2O) 15, 44 (^-CHDCHO) 100
17 $[(M - H)^- - MeOH]$	98 (HD) 12, 82 (HOD) 10, 81 (D_2O) 5, 45 ($^-CD_2CHO$) 100
18 $[(M - H)^- - MeOD]$	98 (H_2) 25, 82 (H_2O) 15, 81 (HOD) 7, 43 ($^-CH_2CHO$) 100
19 $[(M - H)^- - MeOD]$	98 (H_2) 28, 82 (H_2)O 14, 81 (HOD) 6, 43 ($^-CH_2CHO$) 100

[a] Shoulder on main peak, unresolved.

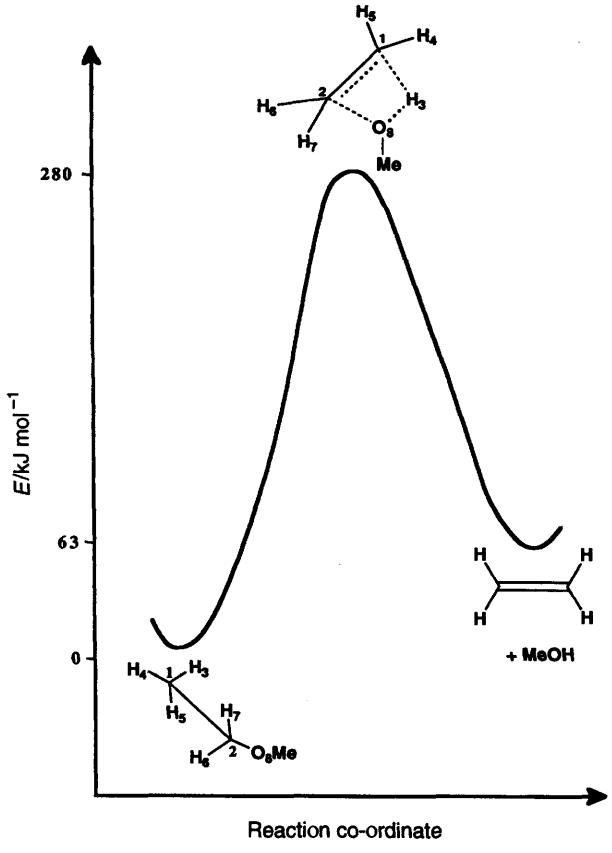

Fig. 3 Pictorial representation of the reaction energetics for the model charge-remote fragmentation mechanism. See the text and Table 3 for full details.

Theoretical studies of mechanistic possibilities (10)–(12)

The experimental evidence outlined above concerning the loss of methanol can be interpreted in terms of any of mechanisms (10)–(12), but the cyclisation process (10) seems the most probable because of the co-occurrence of three processes, *viz.*, the formation of MeO^- and of its solvated counterpart $[MeO^-(H_2O)]$, and the elimination of methanol. In order to investigate further mechanistic scenarios (10)–(12), we now turn to a theoretical study of the problem. Two of the processes [(10) and (12)] have been studied in detail using semiempirical calculations using GAUSSIAN 94[16] and GAMESS-US[17] (see the Experimental section for full details of procedures used).

The elimination of methanol from deprotonated *trans*-4-methoxycyclohexanol to yield the cyclohex-3-enol anion is computed to be endothermic by 48 kJ mol^{-1} (see later) at the AM1 level of theory. We now need to consider (*i*) which of the processes (10)–(12) is most favoured from a kinetic viewpoint, and (*ii*) which process best explains the known products of reaction.

All calculations were performed using the semiempirical AM1 parametric quantum mechanical model.[18–21] The AM1 model was chosen for the calculations reported here because this model has been shown to be generally superior to other popular semi-empirical models, including MNDO and MINDO/3, when studying chemical reactions.[18–21] In particular, predictions of activation energies for simple chemical reactions using AM1 theory are in good agreement with computationally expensive *ab initio* calculations which include allowance for electron correlation.[22,23]

Consider first, the remote reaction [sequence (12), Scheme 1]. The reaction should be synchronous, and the energies the same for each isomer. 1-Methoxyethane has been used as a model system to estimate the activation barrier for the remote reaction sequence. A full geometry optimisation of 1-methoxyethane using the AM1 method shows that although the interaction MeO and H moieties initially assume a staggered configuration, the transition state assumes more of an eclipsed geometry, with an almost entirely planar configuration. A pictorial representation of the reaction energetics as a function of reaction coordinate is shown in Fig. 3: the barrier to reaction (including scaled zero point energies) is 280 kJ mol^{-1}. The reaction endothermicity is 63 kJ mol^{-1}. The computed molecular geometries of the reactant, transition state and products are recorded in Table 3. Table 3 also lists the computed energy and scaled zero-point energy for each compound.

The proton transfer/elimination process (11) (Scheme 1) should be regiospecific and is summarised in formula **20**. The O^- and transferring H must be diaxial, and the H and OMe involved in the elimination should be *anti*. This arrangement is achievable for the *trans* isomer in the diaxial conformation **20** [the overall process is illustrated by arrows in **20**: the actual process is likely to be stepwise, proceeding through an E1cb carbanion intermediate *cf.*, sequence (11), Scheme 1]. The analogous process for the *cis* isomer must be unfavourable in comparison, since it cannot achieve the correct alignment of the H and OMe groups for the *anti* elimination (*cf.*, **21**). We have not computed the activation energies associated with sequence (11): we believe the complex computation required for this multistep process is unnecessary because the key proton transfer step [see sequence (11), Scheme 1 and *cf.*, **20**] is kinetically unfavourable. The latter point is demonstrated as follows: (*i*) for the *trans* isomer, the activation energy required to convert the diequatorial conformer into the required diaxial precursor **20** is at least 40 kJ mol^{-1},[24] and (*ii*) the additional activation

Table 3 Energies and selected geometrical parameters of the optimised structures of Fig. 3[a]

Compound	Energy[b]	ZPE[c]	Bond length[d]		Angle[e]		Dihedral angle[f]	
Reactant	−0.093 80	0.096 83	1–2	1.510(6)	3–1–2	110.39	3–1–2–8	−59.82
			1–3	1.116(1)	4–1–2	109.38	4–1–2–8	−179.98
			1–4	1.115(6)	5–1–2	110.39	5–1–2–8	59.85
			1–5	1.116(1)	6–2–1	111.13	3–1–2–7	−179.16
			2–6	1.123(0)	7–2–1	111.13	4–1–2–7	60.67
			2–7	1.123(0)	8–2–1	106.95	5–1–2–7	−59.50
			2–8	1.427(5)	Me–8–2	112.59	1–2–8–Me	180.0
			2–Me	1.416(6)				
Transition state	0.019 23	0.090 92	1–2	1.429(2)	3–1–2	80.60	4–1–2–8	−103.62
			1–3	1.641(1)	4–1–2	119.80	5–1–2–8	100.53
			1–4	1.093(7)	5–1–2	119.80	4–1–2–6	3.88
			1–5	1.093(4)	6–2–1	119.16	5–1–2–7	−5.42
			2–6	1.108(4)	7–2–1	119.24	1–2–8–3	3.80
			2–7	1.108(4)	8–2–1	90.06	6–2–8–3	−116.54
			2–8	1.574(3)	2–8–3	92.05	7–2–8–3	124.03
			8–3	1.166(2)			4–1–2–7	150.44
Product	−0.063 19	0.101 80	C–C	1.325(9)	C–C–H	122.73	H–C–C–H (*trans*)	179.99
			C–H	1.098(2)			H–C–C–H (*cis*)	0.01
			O–Me	1.413(3)				

[a] Optimized geometries calculated using AM1 semiempirical theory. See the Experimental section for full details. Optimized geometries and atom numbering schemes are shown in Fig. 3. [b] Hartree. [c] Zero-point energy, (Hartree), scaled by 0.89. [d] Å. [e] deg. [f] deg.

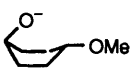

22

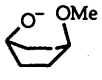

23

energy then required to convert **20** into the E1cb intermediate is likely to be at least 200 kJ mol^{-1} [proton transfer forms a carbanion which we estimate is some 160 kJ mol^{-1} less thermodynamically stable than reactant alkoxide **20**; the ΔG°_{acid} values for models RO*H* and RCH_2R are, respectively, 1564 and 1723 kJ mol^{-1} [25]].

The cyclisation/elimination mechanism [sequence (**10**), Scheme 1] can be effected for the *trans* isomer through boat form **22**; the cyclisation for the *cis* isomer **23** is energetically unfavourable in comparison. The reaction for the more favourable *trans* system has been computed at the AM1 level of theory. The reaction coordinate profile diagram is shown in Fig. 4 commencing with the boat form **22**. We compute that **22** is 15 kJ mol^{-1} less stable than the lowest energy bis-equatorial chair conformer. This gives an overall reaction endothermicity from the bis-equatorial reactant of 48 kJ mol^{-1}. Reactant, transition state, intermediate and product geometries are listed along the reaction coordinate in Fig. 4. All computed molecular geometries, energies and scaled zero point energies are recorded in Table 4.

The initial barrier to reaction is the cyclisation step, with a computed barrier of 181 kJ mol^{-1} from **22**. This barrier is 100 kJ mol^{-1} lower in energy than for the charge-remote fragmentation mechanism illustrated in Fig. 3. The process shown in Fig. 4 involves a stable intermediate along the reaction pathway. The barrier to product formation from the intermediate is 59 kJ mol^{-1}, with the reaction endothermicity from **22** being 33 kJ mol^{-1} (48 kJ mol^{-1} from the bis-equatorial conformer).

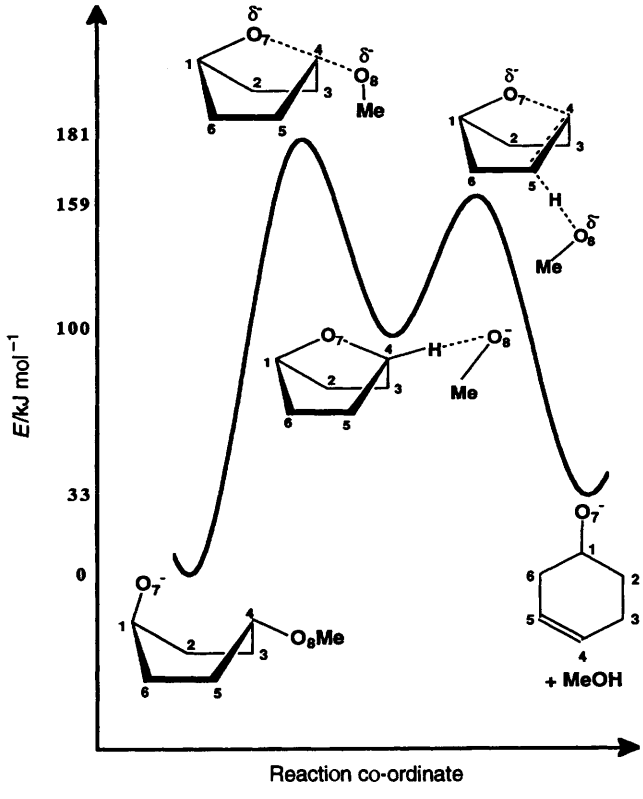

Fig. 4 Pictorial representation of the cyclisation/elimination mechanism (10). See the text and Table 4 for full details.

Conclusions

We now summarise all available data and make the following observations.

(*i*) The remote mechanism [sequence (12)] has a high activation barrier. The energetics of this process should be the same (or very similar) for both *cis* and *trans* isomers, assuming that the 'remote' reaction is independent of the charged centre, and that different orientations of O$^-$ and MeO substituents in the isomers have no steric influence on the reaction. Given this scenario, the peak widths of the product peaks from both isomers should either be the same or very similar. Since the peak widths of the product peaks are significantly different in both spectra, the remote mechanism cannot be the sole process operating for both isomers. In addition, the ion [MeO$^-$(H$_2$O)] cannot arise *via* the remote process since the two interacting groups cannot approach each other during sequence (12).

(*ii*) Proton transfer followed by elimination [process (11)] seems an unlikely possibility. The proton transfer has a significant barrier irrespective of which isomer is involved: the subsequent elimination reaction for the *cis* isomer is additionally unfavourable by the non-availability of an *anti* elimination pathway. The formation of [MeO$^-$(H$_2$O)] cannot be accommodated by this mechanism.

Table 4 Energies and selected geometrical parameters of the optimised structures of Fig. 4[a]

Compound	Energy[b]	ZPE[c]	Bond length[d]		Angle[e]		Dihedral angle[f]	
Reactant	−0.168 55	0.175 18	1–2	1.567	1–2–3	113.02	1–2–3–4	−20.76
			2–3	1.513	2–3–4	109.97	2–3–4–5	66.84
			3–4	1.523	3–4–5	110.64	3–4–5–6	−43.14
			4–5	1.525	4–5–6	110.23	4–5–6–1	−21.51
			5–6	1.513	5–6–1	112.67	7–1–2–3	86.96
			6–1	1.561	7–1–2	113.65	2–3–4–8	−175.27
			1–7	1.315	3–4–8	110.47	7–1–6–5	−62.31
			4–8	1.443	7–1–6	114.45	6–5–4–8	−163.34
Transition state 1	−0.097 94	0.172 98	1–2	1.553	1–2–3	104.08	1–2–3–4	8.35
			2–3	1.531	2–3–4	107.92	2–3–4–5	56.64
			3–4	1.511	3–4–5	114.89	3–4–5–6	−56.86
			4–5	1.512	4–5–6	107.99	4–5–6–1	−8.05
			5–6	1.531	5–6–1	104.03	7–1–2–3	39.48
			6–1	1.553	7–1–2	105.90	2–3–4–8	151.09
			1–7	1.371	3–4–8	91.10	1–7–4–5	−57.45
			7–4	1.940	7–4–8	172.51	1–7–4–8	168.83
			4–8	1.997	1–7–4	90.45	1–7–4–3	57.51
					3–4–8	91.10	3–4–8–Me	162.44
Intermediate	−0.139 11	0.173 06	1–2	1.548	1–2–3	101.91	1–2–3–4	0.22
			2–3	1.541	2–3–4	102.60	2–3–4–5	72.31
			3–4	1.549	3–4–5	107.32	3–4–5–6	−72.38
			4–5	1.548	4–5–6	102.60	4–5–6–1	−0.11
			5–6	1.541	5–6–1	101.92	7–1–2–3	33.61
			6–1	1.548	7–1–2	102.01	4–H–8–Me	−40.06
			1–7	1.453	1–7–4	97.89	1–7–4–5	−55.16
			7–4	1.463	4–H–8	155.17	5–4–H–8	56.70
			4–H	1.128	H–8–Me	106.72	1–7–4–3	55.35
			8–H	1.963	7–4–H	111.38	3–4–H–8	−71.92
			8–Me	1.317				
Transition state 2	−0.104 88	0.171 48	1–2	1.574	1–2–3	102.91	1–2–3–4	12.05
			2–3	1.490	2–3–4	109.40	2–3–4–5	54.83
			3–4	1.402	3–4–5	116.78	3–4–5–6	−58.52
			4–5	1.521	4–5–6	107.49	4–5–6–1	−7.58
			5–6	1.532	5–6–1	102.52	7–1–2–3	34.69
			6–1	1.557	7–1–2	107.70	4–5–H–8	107.85
			1–7	1.378	5–H–8	174.32	1–7–4–5	−61.01
			7–4	1.913	H–8–Me	107.17	6–5–H–8	−5.61
			5–H	1.963	1–7–4	88.93	1–7–4–3	55.96
			8–H	0.992	4–5–H	101.78	5–H–8–Me	−6.04
			8–Me	1.400	6–5–H	103.33	1–6–5–H	119.86
							3–4–5–H	−54.03
Product	−0.150 54	0.169 50	1–2	1.569	1–2–3	115.42	1–2–3–4	7.80
			2–3	1.478	2–3–4	124.07	2–3–4–5	−1.65
			3–4	1.337	3–4–5	122.18	3–4–5–6	24.63
			4–5	1.482	4–5–6	111.53	4–5–6–1	−53.40
			5–6	1.510	5–6–1	111.63	7–1–2–3	93.03
			6–1	1.561	7–1–2	113.83	4–5–H–8	−150.38
			1–7	1.311	7–1–6	114.15	7–1–6–5	−69.55
			5–H	2.458	5–4–H	63.39	5–H–8–Me	−115.83
			4–H	2.746	4–H–8	166.08	3–4–9–8	114.07
			8–H	0.971	H–8–Me	107.15	4–H–8–Me	156.44
			8–Me	1.410	5–H–8	153.61	5–H–8–Me	63.13

[a] Optimized geometries calculated using AM1 semiempirical theory. See the experimental section for full details. Optimized geometries and atom numbering schemes are shown in Fig. 4. [b] Hartree. [c] Zero-point energy (Hartree), scaled by 0.89. [d] Å. [e] deg. [f] deg.

(*iii*) The activation barrier for the slow step of the cyclisation/elimination process of the *trans* isomer [sequence (10)] is computed to be 181 kJ mol^{-1} (from boat form **22**), a value which compares favourably with those of other possible mechanisms. There is a condensed-phase analogy for this process.[12] The cyclisation process enables the O^- and MeO groups to approach each other, and thus of all the possible mechanisms, is best able to explain the formation of $[MeO^-(H_2O)]$.

(*iv*) The cyclisation mechanism [sequence (10)] is expected to be less energetically favourable for the *cis* isomer than for its *trans* counterpart, because of the unfavourable juxtaposition of interacting groups in the *cis* case. The presence of $[MeO^-(H_2O)]$ in the spectrum of the *cis* isomer demands again that the O^- and MeO groups are able to approach closely in this system.

In conclusion, we propose the cyclisation mechanism shown in Scheme 3 to rationalise the elimination of MeOH [eqn. (24)] and the formation of MeO^- [eqn. (25)] and $[MeO^-(MeOH)]$ [eqn. (26)], from the deprotonated form of *trans*-4-methoxycyclohexanol intermediate **A**.† It is likely that a similar mechanism operates for the *cis* isomer, except that the initial

† A reviewer has indicated that the representation **A** in Scheme 3 is confusing since structure **A** neither appears as a transition state nor a reactive intermediate in Fig. 4. In Scheme 3 we are attempting to summarise (in overview) the proposed mechanistic connection in the formation of three related products. Structure **A** (a structure intermediate between the reactive intermediate and transition state 2 of Fig. 4) is used to provide a simple pictorial representation of that mechanistic connectivity.

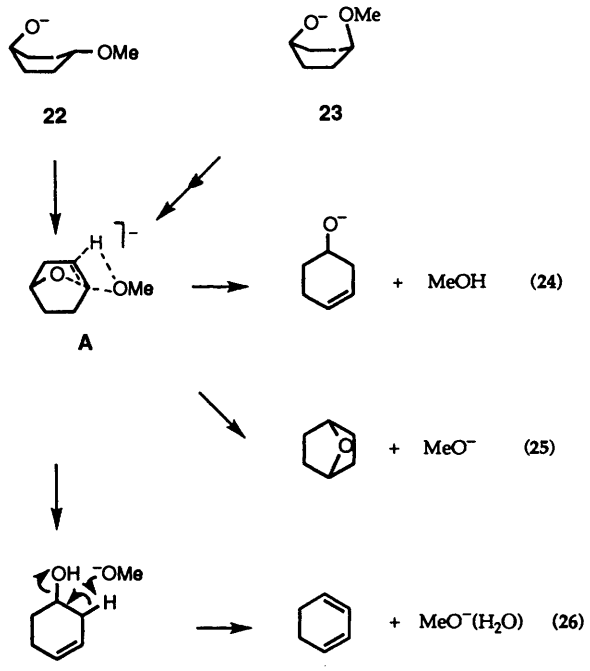

Scheme 3

cyclisation step is less favourable in this case. There is no evidence to indicate the operation of a charge-remote mechanism in either instance.

Experimental

Mass spectrometric methods

Collisional activation (CID) mass spectra (MS/MS) were determined with a VG ZAB 2HF mass spectrometer.[26] Full operating details have been reported.[27] Specific details were as follows: the chemical ionization slit was used in the chemical ionization source, the ionising energy was 70 eV, the ion source temperature was 100 °C, and the accelerating voltage was 7 kV. The liquid samples were introduced through the septum inlet with no heating [measured pressure of sample 1×10^{-6} Torr (1 Torr = 133.322 Pa)]. Deprotonation was effected using HO^- (from H_2O: measured pressure 1×10^{-5} Torr). The estimated source pressure was 10^{-1} Torr. CID MS/MS data were obtained by selecting the particular anion under study with the magnetic sector, passing it through the collision cell, and using the electric sector to separate and monitor the product ions. Argon was used as the collision gas in the second collision cell (measured pressure, outside the cell, 2×10^{-7} Torr), giving a 10% reduction in the main beam, equivalent to single collision conditions. Peak-width measurements were performed with the instrument in MS/MS mode using the electric sector to scan the peak under study. The peak width (at half height), quoted in volts, is a mean of ten individual experiments (the main beam peak width at half height under the instrumental conditions used was 6 V).

MS/MS/MS tandem mass spectra were measured with a MS TA 50 mass spectrometer as described previously.[28] The pressure of He collision gas in both collision cells was 1×10^{-6} Torr, producing a reduction in the main beam of 30%.

Synthesis of labelled and unlabelled compounds

Cyclohexanone was a commercial sample, and cyclohex-3-enol was prepared by a reported procedure.[29]

The stereoisomeric 4-methoxycyclohexanols were prepared as follows. 4-Methoxycyclohexanone was prepared from cyclohexane-1,4-dione monoethylene ketal by a standard procedure.[30] Reduction of 4-methoxycyclohexanone with lithium aluminium hydride in tetrahydrofuran by a reported procedure,[31] gave a mixture of *cis*- and *trans*-4-methoxycyclohexanol in the ratio 3:2 as determined by ^{1}H NMR spectroscopy.[31] The two isomers were separated by three consecutive complexations with lithium aluminium hydride/aluminium chloride by a reported procedure[32] to give the pure *cis*- and *trans*-4-methoxycyclohexanols in the ratio 3:1. Their purity was better than 98% as established by a comparison of their ^{1}H NMR spectra with reported spectra.[32]

Deuterium-labelled compounds

Deuterium incorporation was determined by negative ion mass spectrometry in all cases. All deuterium-labelled compounds were purified by distillation under vacuum.

cis- and *trans*-[3,3,5,5-$^2H_4$]-4-Methoxycyclohexanol

(*a*) Cyclohexane-1,4-dione monoethylene ketal (5 g) was added to NaOD–D_2O [prepared by adding Na (0.3 g) to deuterium oxide (20 cm^3)] at 0 °C. The mixture was allowed to warm to 25 °C, stirred at that temperature for 16 h, and extracted with dichloromethane (5×25 cm^3). The combined organic extract was dried (Na_2SO_4) and concentrated *in vacuo* to yield 4.9 g (95%) of [2,2,6,6-$^2H_4$]cyclohexane-1,4-dione monoethylene ketal 2,2,6,6-D_4 ($^2H_4$ > 96% as determined by negative ion mass spectrometry).

(*b*) The $^2H_4$ ketal (4.9 g) was reduced[33] to [3,3,5,5-$^2H_4$]-4-hydroxycyclohexanone ethylene ketal (4.1 g, 83% yield, $^2H_4$ > 96%) with lithium aluminium hydride in refluxing tetrahydrofuran.

(*c*) The $^2H_4$ alcohol (4.1 g) was methylated with methyl iodide under basic conditions[9] to give [3,3,5,5-$^2H_4$]-4-methoxycyclohexanone ethylene ketal (3.8 g, 85% yield, $^2H_4$ > 96%).

(*d*) The $^2H_4$ methoxy derivative (3.8 g) was reacted[34] with aqueous acetic acid (85% acetic acid) to produce [3,3,5,5-$^2H_4$]-4-methoxycyclohexanone (2.05 g, 72% yield, $^2H_4$ > 96%).

(*e*) The $^2H_4$ methoxycyclohexanone (1.6 g) was reduced with lithium aluminium hydride in tetrahydrofuran by the reported procedure,[31] to yield 1.2 g of a 3:2 mixture of *cis* and *trans* isomers as indicated by ^{1}H NMR spectroscopy. The two isomers were separated by three consecutive complexations with lithium aluminium hydride/aluminium chloride[32] to yield *cis*-[3,3,5,5-$^2H_4$]-4-methoxycyclohexanol (0.15 g, $^2H_4$ > 96%) and *trans*-[3,3,5,5-$^2H_4$]-4-methoxycyclohexanol (0.05 g $^2H_4$ > 96%). The ^{1}H NMR spectra of these compounds indicated that their purity was > 98%.[cf. 32]

trans-[2,2,6,6-$^2H_4$]-4-Methoxycyclohexanol

4-Methoxycyclohexanone was treated with NaOD–D_2O [as in (*a*) above, except that three cycles were used] to yield [2,2,6,6-$^2H_4$]-4-methoxycyclohexanone in near quantitative yield ($^2H_4$ > 99%). Reduction this time using the Li–NH_3 procedure[35] gave a mixture of the *cis* and *trans* products (1:5, as determined by ^{1}H NMR) in 75% yield. The mixture was converted into the tosylates,[36] and several crystallisations (from light petroleum) gave a product which, when hydrolysed,[37] gave *trans*-[2,2,6,6-$^2H_4$]-4-methoxycyclohexanol (15% yield from the initial mixture, $^2H_4$ > 99%), which was shown to be > 95% pure by ^{1}H NMR spectroscopy.[32]

cis-[1-^{2}H]-4-Methoxycyclohexanol

4-Methoxycyclohexanone was reduced using lithium aluminium deuteride–tetrahydrofuran by the reported procedure[31] to yield a 3:1 mixture (as determined by ^{1}H NMR spectroscopy) of the *cis*- and *trans*-[1-^{2}H]-4-methoxycyclohexanol (70% yield, ^2H = 99%). Conversion of this mixture to the tosylates[36] followed by two crystallisations (from light petroleum), then hydrolysis[37] of the product, gave *cis*-[1-^{2}H]-4-methoxycyclohexanol (10% yield from the initial mixture, ^2H = 99%) which was > 95% pure as determined by ^{1}H NMR spectroscopy.[32]

Computational methods

Semiempirical molecular orbital calculations using the AM1

model Hamiltonian[38] were performed with the GAUSSIAN 94[16] and GAMESS-US[17] systems of programs. Calculations were performed on a variety of computational platforms, including DECStation 5000/25 and Silicon Graphics Indigo^2 xZ workstations, as well as Thinking Machines CM-5 and Silicon Graphics Power Challenge supercomputers.

Optimised molecular geometries were characterised as local minima or transition states by subsequent vibrational frequency calculations. Molecular geometries representing local minima possess all positive vibrational frequencies; transition states are identified as possessing one (only) imaginary frequency as well as one (only) negative eigenvalue of the Hessian matrix. The zero-point energy for each structure was also obtained from the frequency calculations. Calculated zero-point energies tend to overestimate actual energies by up to *ca.* 15% and are therefore scaled by 0.89.[39] Reaction barriers were determined by comparing zero point-corrected energies of the various local minima and transition states. Intrinsic Reaction Coordinate (IRC) calculations from each transition state were undertaken to confirm that the calculated transition state geometries do indeed connect the relevant local minima on the overall reaction potential energy surface.

The following computational protocol was employed in this study. Optimised geometries for reactants and products (as well as the intermediate structure shown in Figs. 3 and 4) were determined using GAUSSIAN 94. Molecular geometries of transition states linking local minima on the reaction potential energy surface were then determined using the Linear Synchronous Transit (LST) approach.[40] The structure resulting from an LST calculation was subsequently used as input for a saddle point geometry optimisation using GAMESS. The saddle point geometry determined from the GAMESS calculation was then input, along with the reactant and product geometric specifications, into a QST3 transition-state optimisation using GAUSSIAN 94. QST3 transition-state optimisations employ the Synchronous Transit-Guided Quasi-Newton (STQN) method developed by Schlegel and co-workers.[41] Finally, IRC calculations were used to confirm that computed transition-state geometries do connect the reactants and products of interest.

Acknowledgements

We thank the Australian Research Council for the on-going financial support of our ion chemistry research programmes. S. D. thanks the ARC for a research associate position. We are grateful to Dr R. N. Hayes and Professor M. L. Gross (then at the University of Nebraska, Lincoln) for obtaining the MS/MS/MS data for deprotonated cyclohexanone and cyclohex-3-enol with their MS 50 TA instrument. Supercomputer time and support provided by the South Australia Centre for Parallel Computing (SACPC) is gratefully acknowledged.

References

1 J. Adams, *Mass Spectrom. Rev.*, 1990, **9**, 349, and references cited therein.
2 M. L. Gross, *Int. J. Mass Spectrum. Ion Processes*, 1992, **118/119**, 137 and references cited therein.
3 M. M. Cordero and C. Wesdemiotis, *Anal. Chem.*, 1994, **66**, 861.
4 J. H. Bowie in *Experimental Mass Spectrometry*, ed. D. H. Russell, Plenum Press, New York, 1994, pp. 1–38.
5 P. C. H. Eichinger and J. H. Bowie, *Int. J. Mass Spectrom. Ion Processes*, 1991, **110**, 123; see also M. Claeys and H. Van den Leuvel, *Biol. Mass Spectrom.*, 1994, **23**, 20, and references cited therein.
6 S. Dau and J. H. Bowie, *J. Chem. Soc., Perkin Trans. 2*, 1994, 543.
7 S. Dau and J. H. Bowie, *J. Chem. Soc., Perkin Trans. 2*, 1994, 2097.
8 R. J. Waugh and J. H. Bowie, *Rapid Commun. Mass Spectrom.*, 1994, **8**, 169.
9 S. Dau, R. B. Whait, M. J. Alexander, R. N. Hayes, A. T. Lebedev, P. C. H. Eichinger and J. H. Bowie, *J. Am. Chem. Soc.*, 1993, **115**, 5709.
10 R. G. Cooks, J. H. Beynon, R. M. Caprioli and G. R. Lester, *Metastable Ions*, Elsevier, Amsterdam, 1973, pp. 57–121.
11 W. Tumas, R. F. Foster, M. J. Pellerite and J. I. Brauman, *J. Am. Chem. Soc.*, 1983, **105**, 7474 and references cited therein.
12 H. W. Heine, *J. Am. Chem. Soc.*, 1957, **79**, 6268.
13 G. Wilke and H. Muller, *Justus Liebigs Ann. Chem.*, 1960, **629**, 222.
14 M. J. Raftery and J. H. Bowie, *Int. J. Mass Spectrom. Ion Processes*, 1987, **79**, 267.
15 S. Dua and J. H. Bowie, *Org. Mass Spectrom.*, 1993, **28**, 1155.
16 GAUSSIAN 94, Revision C.3, M. J. Frisch, G. W. Trucks, H. B. Schlegel, P. M. W. Gill, B. G. Johnson, M. A. Robb, J. R. Cheesman, T. Keith, G. A. Petersson, J. A. Montgomery, K. Raghavachari, M. A. Al-Latham, V. G. Zakrzewski, J. V. Ortiz, J. B. Foresman, J. Cioslowski, B. B. Stefanov, A. Nanayakkara, M. Challacombe, C. Y. Peng, P. V. Ayala, W. Chen, M. W. Wong, J. L. Andres, E. S. Replogle, R. Gomperts, R. L. Martin, D. J. Fox, J. S. Binkley, D. J. Defrees, J. Baker, J. P. Stewart, M. Head-Gordon, C. Gonzalez and J. A. Pople, Gaussian Inc., Pittsburgh, PA, 1995.
17 M. W. Schmidt, K. K. Baldridge, J. A. Boatz, S. T. Elbert, M. S. Gordon, J. H. Jensen, S. Koseki, N. Matsunaga, K. A. Nguyen, S. Su, T. L. Windus, M. Depuis and J. A. Montgomery, *J. Comput. Chem.*, 1993, **14**, 1347.
18 M. J. S. Dewar and D. M. Storch, *J. Am. Chem. Soc.*, 1985, **107**, 3898.
19 V. B. Luzhkov and C. A. Venanzi, *J. Phys. Chem.*, 1995, **99**, 2312.
20 W. J. Thiel, *J. Am. Chem. Soc.*, 1981, **103**, 1413.
21 S. Schroeder and W. J. Thiel, *J. Am. Chem. Soc.*, 1986, **108**, 7985.
22 K. Hsu, R. J. Buenker and S. D. Peyerimhoff, *J. Am. Chem. Soc.*, 1971, **93**, 2117.
23 S. Shigeyoshi, Y. Musashi and K. Ohkubo, *J. Am. Chem. Soc.*, 1993, **115**, 1515.
24 D. S. Noyce, *J. Am. Chem. Soc.*, 1962, **84**, 386.
25 J. E. Bartmess, J. A. Scott and R. T. McIver, *J. Am. Chem. Soc.*, 1979, **101**, 6047; C. H. DePuy, V. M. Bierbaum and R. Damrauer, *J. Am. Chem. Soc.*, 1984, **106**, 4051.
26 VG ZAB 2HF, VG Analytical, Manchester, UK.
27 M. B. Stringer, J. L. Holmes and J. H. Bowie, *J. Am. Chem. Soc.*, 1986, **108**, 3888.
28 D. J. Burinsky, R. G. Cooks, E. K. Chess and M. L. Gross, *Anal. Chem.*, 1982, **54**, 295; M. L. Gross, E. K. Chess, P. A. Lyon, F. W. Crow, S. Evans and H. Tudge, *Int. J. Mass Spectrom. Ion Phys.*, 1982, **42**, 243.
29 C. J. Gogek, *Can. J. Chem.*, 1951, **29**, 946.
30 A. Mendelbaum and A. Cais, *J. Org. Chem.*, 1961, **26**, 2633.
31 J. E. Bäckvall, R. E. Nordburg, E. E. Bjorkman and C. Moberg, *J. Chem. Soc., Chem. Commun.*, 1980, 943.
32 E. L. Eliel and T. J. Brett, *J. Org. Chem.*, 1963, **28**, 1923.
33 A. Burger, L. Turnbull and J. G. Dinwiddie, *J. Am. Chem. Soc.*, 1950, **72**, 5512.
34 D. J. Goldsmith and I. Sakarno, *J. Org. Chem.*, 1976, **41**, 2095.
35 M. Hudlicky, *Reductions in Organic Chemistry*, Wiley, New York, 1984, p. 25.
36 A. I. Vogel, *Practical Organic Chemistry*, Longman and Green, London, 1956, 3rd edn., p. 684.
37 P. Ruggli, J. Leupin and A. Businger, *Helv. Chim. Acta*, 1941, **24**, 339.
38 M. J. S. Dewar, E. G. Zoebisch and E. F. Healy, *J. Am. Chem. Soc.*, 1985, **107**, 3902.
39 W. Hehre, L. Radom, P. v. R. Schleyer and J. A. Pople, *Ab Initio Molecular Orbital Theory*, Wiley, New York, 1986.
40 T. A. Halgren and W. N. Lipscomb, *Chem. Phys. Lett.*, 1977, **49**, 225.
41 C. Peng and H. B. Schlegel, *Isr. J. Chem.*, 1993, **33**, 449.

Paper 6/01663D
Received 8*th March* 1996
Accepted 30*th May* 1996